Available online at www.sciencedirect.com
ScienceDirect
Bioorganic & Medicinal Chemistry 14 (2006) 8608–8621
Bioorganic & Medicinal Chemistry

Synthesis, dihydrofolate reductase inhibition, antitumor testing, and molecular modeling study of some new 4(3*H*)-quinazolinone analogs

Sarah T. Al-Rashood,[a] Ihsan A. Aboldahab,[a] Mahmoud N. Nagi,[b] Laila A. Abouzeid,[a] Alaa A. M. Abdel-Aziz,[a] Sami G. Abdel-hamide,[a] Khairia M. Youssef,[a] Abdulrahman M. Al-Obaid[a] and Hussein I. El-Subbagh[a,*]

[a]*Department of Pharmaceutical Chemistry, College of Pharmacy, King Saud University, PO Box 2457, Riyadh 11451, Saudi Arabia*
[b]*Department of Pharmacology, College of Pharmacy, King Saud University, PO Box 2457, Riyadh 11451, Saudi Arabia*

Received 26 June 2006; revised 17 August 2006; accepted 21 August 2006
Available online 12 September 2006

Abstract—In order to produce potent new leads for anticancer drugs, a new series of quinazoline analogs was designed to resemble methotrexate (MTX, **1**) structure features and fitted with functional groups believed to enhance inhibition of mammalian DHFR activity. Molecular modeling studies were used to assess the fit of these compounds within the active site of human DHFR. The synthesized compounds were evaluated for their ability to inhibit mammalian DHFR in vitro and for their antitumor activity in a standard in vitro tissue culture assay panel. Compounds **28**, **30**, and **31** were the most active DHFR inhibitors with IC_{50} values of 0.5, 0.4, and 0.4 μM, respectively. The most active antitumor agents in this study were compounds **19**, **31**, **41**, and **47** with median growth inhibitory concentrations (GI_{50}) of 20.1, 23.5, 26.7, and 9.1 μM, respectively. Of this series of compounds, only compound **31** combined antitumor potency with potent DHFR inhibition; the other active antitumor compounds (**19**, **41**, and **47**) all had DHFR IC_{50} values above 15 μM, suggesting that they might exert their antitumor potency through some other mode of action. Alternatively, the compounds could differ significantly in uptake or concentration within mammalian cells.

1. Introduction

Dihydrofolate reductase (DHFR) is an enzyme of pivotal importance in biochemistry and medicinal chemistry. DHFR catalyzes the reduction of folate or 7,8-dihydrofolate to tetrahydrofolate and intimately couples with thymidylate synthase (TS). Inhibition of DHFR or TS activity in the absence of salvage leads to 'thymineless death.' [1–3] Compounds that inhibit DHFR exhibit an important role in clinical medicine as exemplified by the use of methotrexate (MTX, **1**) in neoplastic diseases,[4,5] inflammatory bowel diseases,[6] and rheumatoid arthritis,[7] as well as in psoriasis,[8,9] and in asthma.[10] A new generation of potent lipophilic DHFR inhibitors such as trimetrexate (TMQ, **2**) and piritrexim (PTX, **3**) have shown antineoplastic[11–13] and antifungal[14] activities (Chart 1).

A new series of quinazoline analogs is designed to possess a sulfhydryl or thioether function at position

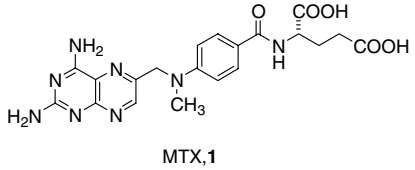

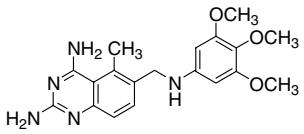

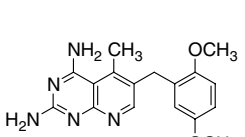

Chart 1.

Keywords: 4(3*H*)-Quinazolinone; DHFR inhibitors; Antitumor activity; Molecular modeling studies.
* Corresponding author. Tel.: +966 1 467 7366; fax: +966 1 467 6383; e-mail: subbagh@yahoo.com

0968-0896/$ - see front matter © 2006 Elsevier Ltd. All rights reserved.
doi:10.1016/j.bmc.2006.08.030

2-, an alkyl, aryl or arylalkyl group at position 3-, a nitro or amino functional group at position 6-, (**5**–**15**). The 6-amino function was used to introduce Schiff's base (**16**–**21**), sulfonamide, amide or thioureido (**34**–**57**) functions. Schiff's bases were utilized to produce compounds **28**–**33**, which carry N–CH_3 side chain in resemblance to MTX (**1**). Thioether,[15] sulfonamide, Schiff's base, and amide and thioureido[16] functional groups are known to contribute to the enhancement of the antitumor activity. Combining the inherent DHFR inhibition activity of the quinazolines[16–24] and those functional groups in one structure was expected to produce more active compounds. Most of those functional groups are also known to increase lipid solubility.[25–28] The present study is a continuation of our previous efforts[29–33] aiming to create novel synthetic lead compound(s) and its in vitro testing for future development as DHFR inhibitor(s).

2. Chemistry

The synthetic strategy to synthesize the targets **5**–**57** is depicted in Schemes 1 and 2. Nitroanthranilic acids (**4a**,**b**) were allowed to react with ethyl, phenyl, and benzyl isothiocyanates to produce 2-thioxo-3-substituted-6 or 7-nitro-3*H*-quinazolin-4-ones (**5**–**8**) adopting reported procedure.[32,33] The 2-thioxo function of **5**–**8** was then methylated using methyl iodide to give the *S*-methyl thioether derivatives **9**–**12**. The 6- or 7-nitro function of **9**–**12** was subjected to metal reduction using Fe/HCl to

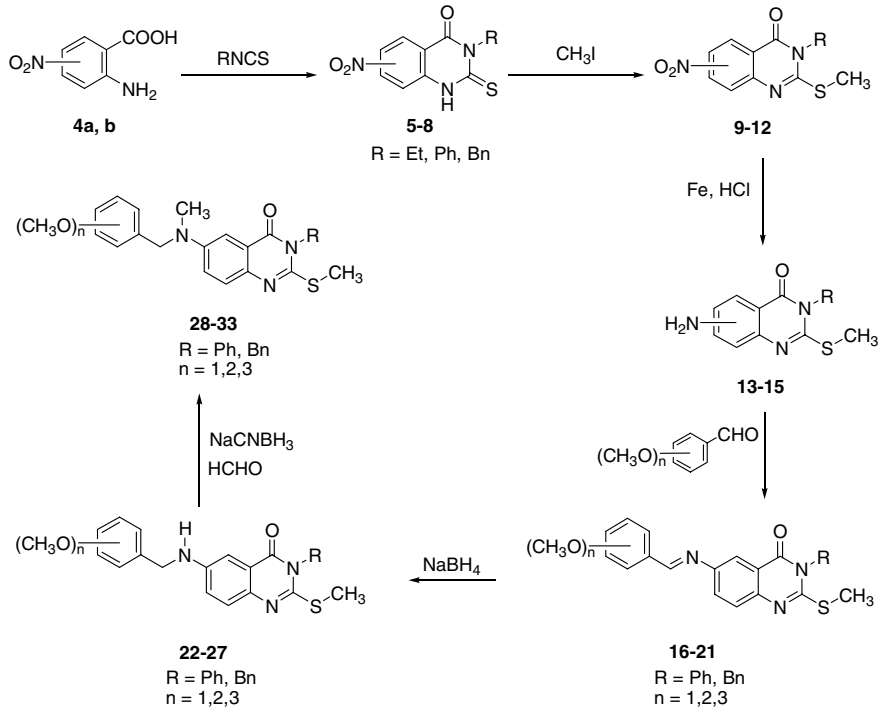

Scheme 1.

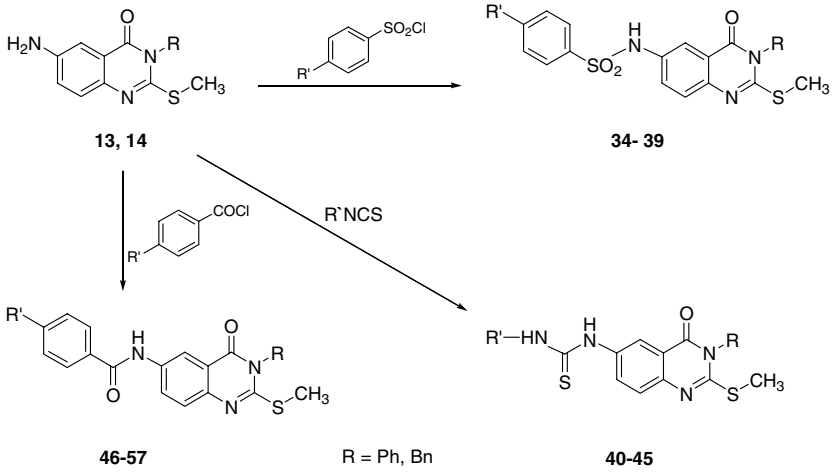

Scheme 2.

Table 1. Physicochemical properties and DHFR inhibition (IC_{50}, μM) of the newly synthesized compounds **5–33**

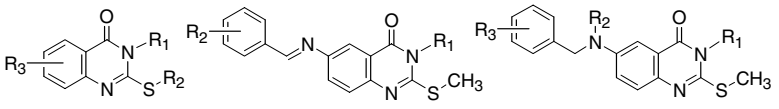

5-15 **16-21** **22-33**

Compound	R_1	R_2	R_3	Yield (%)	Mp (°C)	Solvent	Molecular[a] formula	*m/z* (%)	IC_{50} (μM)
5	Et	H	6-NO_2	69	269–271	EtOH/H_2O	$C_{10}H_9N_3O_3S$	251 (100)	20.0
6	Ph	H	6-NO_2	78	>300	EtOH	$C_{14}H_9N_3O_3S$	299 (84)	30.0
7	Bn	H	6-NO_2	—	—	—	Ref. 37	—	20.0
8	Bn	H	7-NO_2	32	220–222	EtOH/H_2O	$C_{15}H_{11}N_3O_3S$	313 (48)	30.0
9	Et	CH_3	6-NO_2	82	130–132	EtOH	$C_{11}H_{11}N_3O_3S$	265 (30)	25.0
10	Ph	CH_3	6-NO_2	89	200–202	MeOH	$C_{15}H_{11}N_3O_3S$	313 (100)	25.0
11	Bn	CH_3	6-NO_2	—	—	—	Ref. 37	—	25.0
12	Bn	CH_3	7-NO_2	92	139–141	EtOH/$CHCl_3$	$C_{16}H_{13}N_3O_3S$	327 (62)	30.0
13	Ph	CH_3	6-NH_2	28	175–176	EtOH/$CHCl_3$	$C_{15}H_{13}N_3OS$	283 (100)	50.0
14	Bn	CH_3	6-NH_2	32	210–212	EtOH/$CHCl_3$	$C_{16}H_{15}N_3OS$	297 (73)	10.0
15	Bn	CH_3	7-NH_2	36	160–162	EtOH/$CHCl_3$	$C_{16}H_{15}N_3OS$	297 (60)	50.0
16	Ph	4-OCH_3	—	75	220–222	DMF	$C_{23}H_{19}N_3O_2S$	401 (3)	2.0
17	Bn	4-OCH_3	—	62	109–110	DMF	$C_{24}H_{21}N_3O_2S$	415 (10)	10.0
18	Ph	3,4-$(OCH_3)_2$	—	59	118–120	DMF/H_2O	$C_{24}H_{21}N_3O_3S$	431 (6)	50.0
19	Bn	3,4-$(OCH_3)_2$	—	45	133–135	DMF/H_2O	$C_{25}H_{23}N_3O_3S$	445 (1)	40.0
20	Ph	3,4,5-$(OCH_3)_3$	—	67	113–115	DMF	$C_{25}H_{23}N_3O_4S$	461 (1)	13.0
21	Bn	3,4,5-$(OCH_3)_3$	—	73	188–190	DMF	$C_{26}H_{25}N_3O_4S$	475 (4)	20.0
22	Ph	H	4-OCH_3	48	120–122	EtOH/Hex	$C_{23}H_{21}N_3O_2S$	403 (9)	25.0
23	Bn	H	4-OCH_3	72	131–133	EtOH/Hex	$C_{24}H_{23}N_3O_2S$	417 (7)	10.0
24	Ph	H	3,4-$(OCH_3)_2$	65	188–190	EtOH/Hex	$C_{24}H_{23}N_3O_3S$	433 (11)	20.0
25	Bn	H	3,4-$(OCH_3)_2$	53	174–175	EtOH/Hex	$C_{25}H_{25}N_3O_3S$	447 (14)	15.0
26	Ph	H	3,4,5-$(OCH_3)_3$	81	138–140	EtOH/Hex	$C_{25}H_{25}N_3O_4S$	463 (10)	30.0
27	Bn	H	3,4,5-$(OCH_3)_3$	85	152–154	EtOH/Hex	$C_{26}H_{27}N_3O_4S$	477 (3)	30.0
28	Ph	CH_3	4-OCH_3	64	185–187	$CHCl_3$/Hex	$C_{24}H_{23}N_3O_2S$	417 (6)	1.0
29	Bn	CH_3	4-OCH_3	75	172–174	$CHCl_3$/Hex	$C_{25}H_{25}N_3O_2S$	431 (1)	0.5
30	Ph	CH_3	4-OCH_3	72	202–204	$CHCl_3$/Hex	$C_{25}H_{25}N_3O_3S$	447 (8)	0.4
31	Bn	CH_3	4-OCH_3	72	123–125	$CHCl_3$/Hex	$C_{26}H_{27}N_3O_3S$	461 (15)	0.4
32	Ph	CH_3	3,4-$(OCH_3)_2$	92	104–106	$CHCl_3$/Hex	$C_{26}H_{27}N_3O_4S$	477 (9)	1.0
33	Bn	CH_3	3,4-$(OCH_3)_2$	90	72–75	$CHCl_3$/Hex	$C_{27}H_{29}N_3O_4S$	491 (4)	10.0

[a] Analyzed for C, H, N; results are within ±0.4% of the theoretical values for the formulae given.

afford the corresponding 6- or 7-amino compounds **13–15** (Scheme 1 and Table 1). The amino function of compounds **13** and **14** was then reacted with 4-methoxy-, 3,4-dimethoxy-, and 3,4,5-trimethoxybenzaldehyde in boiling DMF to afford the benzylidineamino analogs **16–21**. The formed azomethine function was then subjected to $NaBH_4$ reduction to produce the secondary amines **22–27**, which were then subjected to the reductive methylation process using formaldehyde and $NaCNBH_3$ to produce the N-methylated tertiary amines, 6-[N-(substituted benzyl)-*N*-methyl-amino]-3*H*-quinazolin-4-ones (**28–33**) (Scheme 1 and Table 1). The 2-methylthio-3-(phenyl or benzyl)-6-amino-3*H*-quinazolin-4-ones (**13** and **14**) were reacted with a variety of substituted benzenesulfonyl chlorides producing the 6-sulfonamido analogs **34–39** (Scheme 2 and Table 2). The benzene sulfonamide moiety is carrying 4-CH_3 or 4-Br function that represents electron-donating and electron-withdrawing groups, respectively, in order to evaluate their electronic effects on biological activity. The amino function of **13** and **14** was also reacted with ethyl, phenyl or benzyl isothiocyanates to yield the 6-thioureido analogs **40–45** (Scheme 2 and Table 2). Compounds **13** and **14** were reacted with a variety of substituted benzoyl chlorides to produce the 6-acylamino-derivatives **46–57**, adopting the same reaction conditions used to prepare the 6-sulfonamido analogs **34–39** (Scheme 2 and Table 2). Structure elucidation of the synthesized intermediates and final products was attained by the aid of elementary analyses (C, H and N), NMR, and mass spectrometry.

3. Results and discussion

The synthesized compounds (**5–57**) were evaluated as DHFR inhibitors following a reported procedure,[16] using MTX (**1**) as a positive control. Results are reported as IC_{50} values (Tables 1 and 2). Compounds **16**, **28–32**, **34**, and **36** proved to be the most active DHFR inhibitors in this investigation with IC_{50} values of 2.0, 1.0, 0.5, 0.4, 0.4, 1.0, 2.0, and 2.0 μM, respectively. Compounds **37**, **39**, **42**, **45**, **49**, **51**, and **55** showed moderate inhibition activity with IC_{50} values of 5.0, 7.0, 5.0, 8.0, 8.0, 7.0 and 8.0 μM, respectively; while compounds **14**, **17**, **23**, **33**, **35**, **38**, **43**, **44**, **50**, and **53** showed an equal IC_{50} value of 10 μM.

The synthesized compounds were also subjected to the NCI's in vitro, one dose primary anticancer assay, using

Table 2. Physicochemical properties and DHFR inhibition (IC_{50}, μM) of the newly synthesized compounds **34–57**

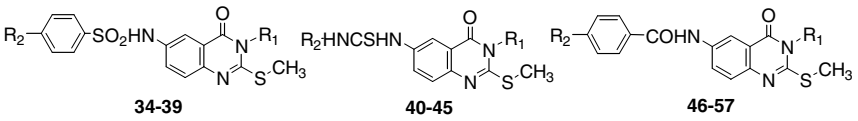

Compound	R_1	R_2	Yield (%)	Mp (°C)	Solvent	Molecular[a] formula	*m/z* (%)	IC_{50} (μM)
34	Ph	H	82	112–114	MeOH	$C_{21}H_{17}N_3O_3S_2$	423 (2)	2.0
35	Bn	H	86	188–190	EtOH	$C_{22}H_{19}N_3O_3S_2$	437 (4)	10.0
36	Ph	Br	91	240–242	EtOH/H_2O	$C_{21}H_{16}BrN_3O_3S_2$	502 (1)	2.0
37	Bn	Br	79	258–260	EtOH/H_2O	$C_{22}H_{18}BrN_3O_3S_2$	516 (1)	5.0
38	Ph	CH_3	88	186–188	MeOH	$C_{22}H_{19}N_3O_3S_2$	437 (5)	10.0
39	Bn	CH_3	94	202–204	MeOH/H_2O	$C_{23}H_{21}N_3O_3S_2$	451 (8)	7.0
40	Ph	Et	84	221–222	EtOAc	$C_{18}H_{18}N_4OS_2$	370 (2)	50.0
41	Bn	Et	89	169–170	EtOAc	$C_{19}H_{20}N_4OS_2$	375 (2)	20.0
42	Ph	Ph	93	123–125	$CHCl_3$/EtOH	$C_{22}H_{18}N_4OS_2$	418 (4)	5.0
43	Bn	Ph	96	195–197	$CHCl_3$/EtOH	$C_{23}H_{20}N_4OS_2$	432 (2)	10.0
44	Ph	Bn	78	215–216	$CHCl_3$/EtOH	$C_{23}H_{20}N_4OS_2$	432 (1)	10.0
45	Bn	Bn	81	203–205	$CHCl_3$/EtOH	$C_{24}H_{22}N_4OS_2$	446 (1)	8.0
46	Ph	H	65	118–120	EtOAc	$C_{22}H_{17}N_3O_2S$	387 (6)	20.0
47	Bn	H	58	192–195	EtOAc	$C_{23}H_{19}N_3O_2S$	401 (8)	15.0
48	Ph	4-Br	73	>300	$CHCl_3$/Hex	$C_{22}H_{16}BrN_3O_2S$	466 (2)	50.0
49	Bn	4-Br	86	>300	$CHCl_3$/Hex	$C_{23}H_{18}BrN_3O_2S$	480 (1)	8.0
50	Ph	4-CH_3	78	125–127	DMF	$C_{23}H_{19}N_3O_2S$	401 (4)	10.0
51	Bn	4-CH_3	82	238–240	DMF	$C_{24}H_{21}N_3O_2S$	415 (1)	7.0
52	Ph	4-OCH_3	90	214–216	DMF	$C_{23}H_{19}N_3O_3S$	417 (1)	70.0
53	Bn	4-OCH_3	64	105–107	DMF	$C_{24}H_{21}N_3O_3S$	431 (7)	10.0
54	Ph	3,4-$(OCH_3)_2$	65	148–150	$CHCl_3$/EtOH	$C_{24}H_{21}N_3O_4S$	447 (2)	40.0
55	Bn	3,4-$(OCH_3)_2$	78	202–203	$CHCl_3$/EtOH	$C_{25}H_{23}N_3O_4S$	461 (3)	8.0
56	Ph	3,4,5-$(OCH_3)_3$	82	238–240	$CHCl_3$/EtOH	$C_{25}H_{23}N_3O_5S$	477 (6)	15.0
57	Bn	3,4,5-$(OCH_3)_3$	87	115–117	$CHCl_3$/EtOH	$C_{26}H_{25}N_3O_5S$	491 (5)	12.0

[a] Analyzed for C, H, N; results are within ±0.4% of the theoretical values for the formulae given.

a 3-cell line panel consisting of MCF-7 (breast), NCI-H460 (lung), and SF-268 (CNS) cancers. Compounds which reduce the growth of any one of the cell lines to 32% or less are passed on for evaluation in the full panel of 60 cell lines over a 5-log dose range.[34–36] Three response parameters, median growth inhibition (GI_{50}), total growth inhibition (TGI), and median lethal concentration (LC_{50}), were calculated for each cell line, using the known drug Melphalan as a positive control. The NCI antitumor drug discovery screen has been designed to distinguish between broad-spectrum antitumor and tumor or subpanel-selective compounds.[37] In the present study, compounds **15**, **19**, **31**, **41**, and **47** passed primary anticancer assay at an arbitrary concentration of 100 μM. Consequently, those active compounds were carried over and tested against a panel of 60 different tumor cell lines. The tested quinazoline analogs showed a distinctive potential pattern of selectivity as well as a broad-spectrum antitumor activity. With regard to sensitivity against individual cell lines, compound **19** showed GI_{50} effectiveness against leukemia CCRF-CEM and SR; melanoma SK-MEL-5 cell lines at concentrations of 1.0, 0.2, and 2.0 μM, respectively. Compound **31** showed GI_{50} activity against leukemia RPMI-8226, SR; melanoma SK-MEL-5 cell lines at concentrations of 2.9, 1.6, and 2.9 μM, respectively. Compound **47** proved to be active at GI_{50} level against colon HCT-116, ovarian OVCAR-3, and renal SN12C cell lines at concentrations of 3.3, 4.3, and 2.4 μM, respectively. With regard to broad-spectrum antitumor activity, the tested compounds showed GI_{50}, TGI, and LC_{50} (MG-MID) values < 100 μM, against leukemia,

Table 3. Median growth inhibitory concentration (GI_{50}, μM) of in vitro subpanel tumor cell lines

Compound	Subpanel tumor cell lines[a]									MG-MID[b]
	I	II	III	IV	V	VI	VII	VIII	IX	
15	27.7	44.6	56.5	43.4	54.3	59.2	34.8	22.4	32.1	34.4
19	12.5	26.4	31.8	37.9	18.8	42.1	22.2	24.1	21.8	20.1
31	8.7	48.2	65.1	28.4	40.4	54.9	20.4	20.7	40.4	23.5
41	15.8	29.5	27.8	33.0	27.1	43.0	28.0	33.3	25.6	26.7
47	6.7	18.4	8.2	23.2	17.2	21.2	10.0	20.7	18.8	9.1
Melphalan	20.1	38.5	42.1	17.1	31.9	43.0	34.4	34.7	39.2	27.1

[a] I, leukemia; II, non-small cell lung cancer; III, colon cancer; IV, CNS cancer; V, melanoma; VI, ovarian cancer; VII, renal cancer; VIII, prostate cancer; IX, breast cancer.

[b] GI_{50} full panel mean-graph midpoint (μM).

Table 4. Total growth inhibitory concentration (TGI, μM) of in vitro subpanel tumor cell lines

Compound	Subpanel tumor cell lines[a]									MG-MID[b]
	I	II	III	IV	V	VI	VII	VIII	IX	
15	76.2	92.3	[c]	91.8	92.2	[c]	92.2	95.2	89.6	90.4 ([c])[d]
19	52.8	80.5	90.7	91.7	61.3	82.2	73.6	87.1	77.2	68.0 (97.8)[d]
31	[c]	89.7	[c]	79.9	75.1	93.8	69.5	[c]	[c]	83.1 ([c])[d]
41	59.2	90.5	71.4	86.3	63.2	84.8	75.8	[c]	69.3	74.7 (97.8)[d]
47	[c]	50.8	64.5	41.7	48.1	40.6	30.3	87.2	45.7	39.5 (78.1)[d]

[a] For subpanel tumor cell lines, see footnote a of Table 3.
[b] TGI full panel mean-graph midpoint (μM).
[c] Compound showed values >100 μM.
[d] Median lethal concentrations (LC_{50}, μM) are shown in parentheses, Melphalan TGI and LC_{50} MG-MID values are 35.3 and 65.5 μM, respectively.

non-small cell lung, colon, CNS, melanoma, ovarian, renal, prostate, and breast cancer subpanel cell lines. Compounds **15** and **31** showed (MG-MID) values <100 μM at only the GI_{50} and TGI levels, while compounds **19**, **41**, and **47** showed potency at the three levels of activity GI_{50}, TGI, and LC_{50} (Tables 3 and 4). Compound **47** proved to be the most active member in this study with GI_{50}, TGI and LC_{50} values of 9.1, 39.5, and 78.1 μM, respectively.

3.1. Molecular modeling study

As an attempt to gain a better insight into the molecular structures of the active compounds **16**, **28**–**32**, **34**, **36**, **37**, and **42**, and the inactive compounds **5**–**13** and **15**, in comparison to MXT (**1**), conformational analysis has been formed by use of the MM+ force-field (calculations in vacuo, bond dipole option for electrostatics, Polak–Ribiere algorithm, and RMS gradient of 0.01 kcal/Å mol)[38] as implemented in HyperChem 6.0.[39] The most stable conformer was fully optimized with Amber force-field[40] followed by AM1 semi-empirical molecular orbital calculation.[41] The global minimum was confirmed as true minimum not saddle point by the absence of negative eigenvalue of the Hessian through frequency calculation. The calculations showed that, compounds **16**, **28**–**32**, **34**, **36**–**37**, and **42** exhibited strong structural similarity to **1** as indicated by their molecular parameters (Table 5). The lowest energy-minimized structures exhibited a common arrangement of the aryl groups (ring **A** and **B**, Figs. 1–3 and 5) around the quinazoline core. Ring **A** was out of the plane of quinazoline ring (torsional angles were 91° and 71° in case of the 3-phenyl and 3-benzyl moieties, respectively). The benzyl group

Table 5. Molecular parameters of the active and the inactive compounds compared with MTX (**1**)

Compound	C log *P*[a]	*R*[b]	*P*[c]	*V*[d]	SA[e]	*D*[f]	IC_{50}[g]
5	1.8	64.1	24.2	658.2	410.9	4.8	20
6	3.2	79.1	30.2	767.6	471.7	4.4	30
7	3.0	83.9	32.0	814.0	495.1	4.8	20
8	3.0	83.9	32.0	815.8	491.3	4.8	20
9	2.1	68.9	26.1	716.2	443.2	5.1	25
10	3.6	83.9	32.0	830.7	507.1	5.8	25
11	3.3	88.8	33.9	871.2	521.9	5.0	25
12	3.3	88.8	33.9	872.2	523.9	5.2	30
13	3.3	82.3	32.0	803.2	486.7	5.2	50
15	3.0	87.2	33.4	846.5	509.1	5.8	50
MTX (**1**)	0.5	118.8	46.1	1200.8	704	8.8	0.001
16	5.2	117.4	45.1	1144.3	681.2	5.4	2.0
28	6.0	123.1	47.4	1199.4	700.7	5.3	1.0
29	5.8	128.0	49.2	1241.6	715.27	3.4	0.5
30	5.8	129.6	49.8	1275.4	738.8	4.8	0.4
31	5.5	134.4	51.7	1316.9	759.9	3.1	0.4
32	5.4	136.1	52.3	1353.9	783.7	5.2	1.0
34	4.7	116.2	42.4	1110.6	658.9	9.9	2.0
36	5.6	123.9	45.0	1175.5	690.3	10.6	2.0
37	5.4	128.7	46.8	1216.6	710.7	8.6	5.0
42	4.6	122.6	47.6	1141.7	668.2	2.7	5.0

[a] (C log *P*) values were calculated by using the CS ChemDraw Ultra version 7.
[b] Refractometry (Å^3).
[c] Polarizability (Å^3).
[d] Molecular volume (Å^3).
[e] Surface area; gride (Å^3).
[f] Dipole moment (Debye).
[g] Data were taken from Tables 1 and 2.

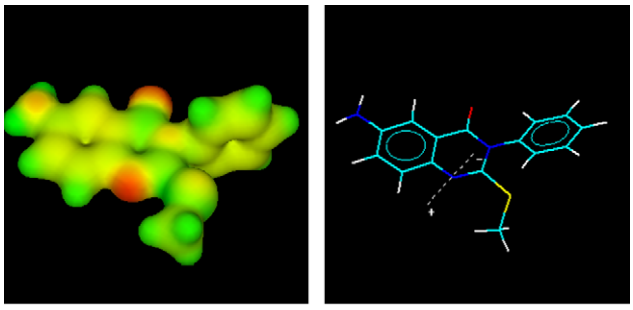

Compound **13**

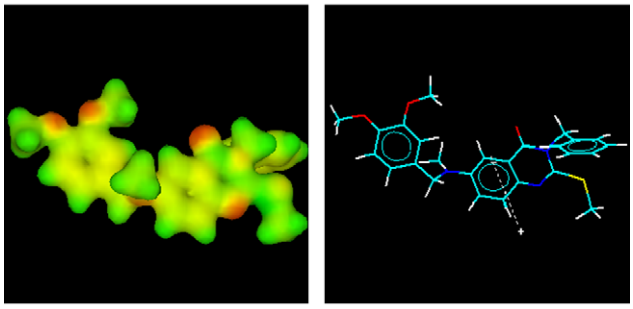

Compound **31**

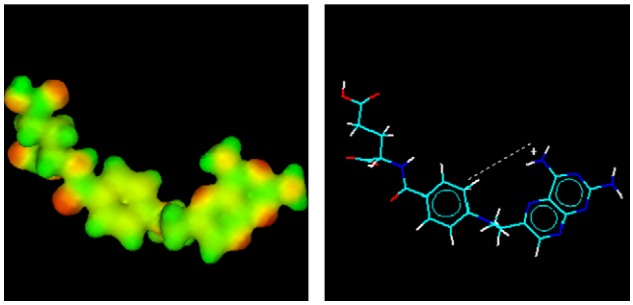

MTX (**1**)

Figure 1. Global minima of compounds **13**, **31** and MTX (**1**) with their dipole moment vector and electrostatic potential isosurface, negative region colors red and positive region colors green.

Figure 3. RMS fit overlay of the active compound **31** (green) and MTX, **1** (violet).

(ring **B**) was deviated from the plane of quinazoline ring by −65° and arranged itself parallel with quinazoline ring. Moreover, the freely rotated methoxy groups were arranged in spatial manner approximately coplanar and parallel with the aryl edges.[42] Similarly, the Ring **B** of **1** arranged itself parallel with pteridine ring and deviated from its plane by −67° (Figs. 3 and 5).

Further evidence of structural similarity and analogy of binding of the most active compounds (**28**–**32**) and MTX (**1**) was obtained from the QSAR-data using the conformations depicted in Figure 1. Semi-empirical calculations of the conformers demonstrated the closely related charge distribution and electrostatic potentials suggesting a similar interaction of those molecules with the potential protein binding site. QSAR studies showed an optimum hydrophobicity (C log *P*) range of 5.2–6.0

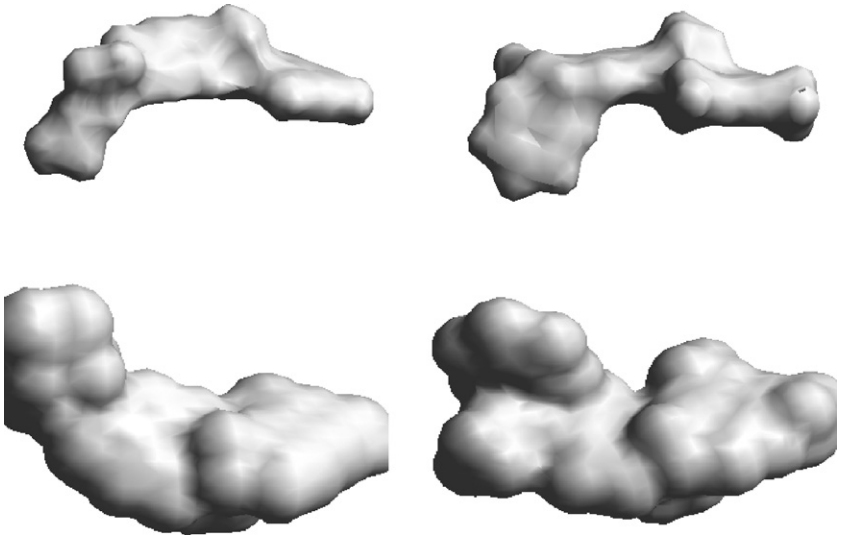

Figure 2. Connolly molecular surface (upper panel) and solvent accessible surface (lower panel) of MTX, **1** (left) and the active compound **31** (right).

for the active compounds, and Clog *P* range of 1.8–3.3 for the inactive compounds. Direct correlation could be established between the Clog *P* and hDHFR inhibition of these series while it could not be correlated with **1** as its Clog *P* value is 0.5 (Table 5). It becomes apparent that Clog *P* values are not the sole predicting factor for biological activity in this study. In addition, despite the variation of the molecular shapes of these ligands, measurements of global molecular parameters such as surface area, volume, and refractivity (Fig. 1) also reflect their similarity to **1**. As shown from Table 5, the biological inefficacy of the inactive compounds **5**–**15** could be attributed to the difficulty to cross the biological membranes due to their physicochemical properties which prevent their access to the putative cavity. Furthermore, semi-empirical calculations of the conformers displayed in Figure 2 described the Connolly molecular surface, solvent accessible surface, and the electrostatic binding characteristics of the surface of the molecules and demonstrated their closely related molecular surface, charge distribution, and electrostatic potential, suggesting a similar interaction of those molecules and compound **1** with the potential hDHFR binding site. Moreover, the energy-minimized conformer **31** and MTX (**1**), as a representative example, were superimposed in order to reveal the similarities and the differences in their structures (Fig. 3). The overlay fitting was carried out with respect to quinazoline and pteridine rings. The results showed that deviation of the superimposed structures was observed in the region of the 6-amphiphilic moiety with rms value of 0.05 Å. This is in addition to what was displayed in Figure 1 which demonstrated the closely related charge distribution and electrostatic potential. Accordingly compounds **31** and **1** could adopt conformations that have close distances and orientations of the assumed major hDHFR-binding groups and showed sufficient agreement of the overall structure electrostatic potential pattern.

The synthesized target compounds have been comparatively evaluated in terms of their binding mode to human dihydrofolate reductase (hDHFR) pocket. Molecular docking and molecular dynamic (MD) simulations have been formed for the proposed compounds (**5**–**57**), to evaluate their recognition profiles at the hDHFR-binding pocket.[43,44] Studying the pteridine ring H-bonding interaction of **1** with the hDHFR active site revealed that the nitrogen atoms at N^1, N^8 and the nitrogen atom of the 2-amino group contributed three stable H-bonds with the key pocket residue Glu30. Besides, the nitrogen atom of the 4-amino group of the pteridine ring conferred trifurcated H-bonds with the 'catalytic triad' residues of hDHFR pocket Ile7, Tyr121, and Val115. Furthermore, the nitrogen and oxygen of the glutamine amide function formed two H-bonds with Asn64 (Fig. 4). Similarly, the binding mode of the investigated quinazolines was formed. In general, the nitrogen atom at $N^1$and the 2-sulfur atom of the quinazoline analogs

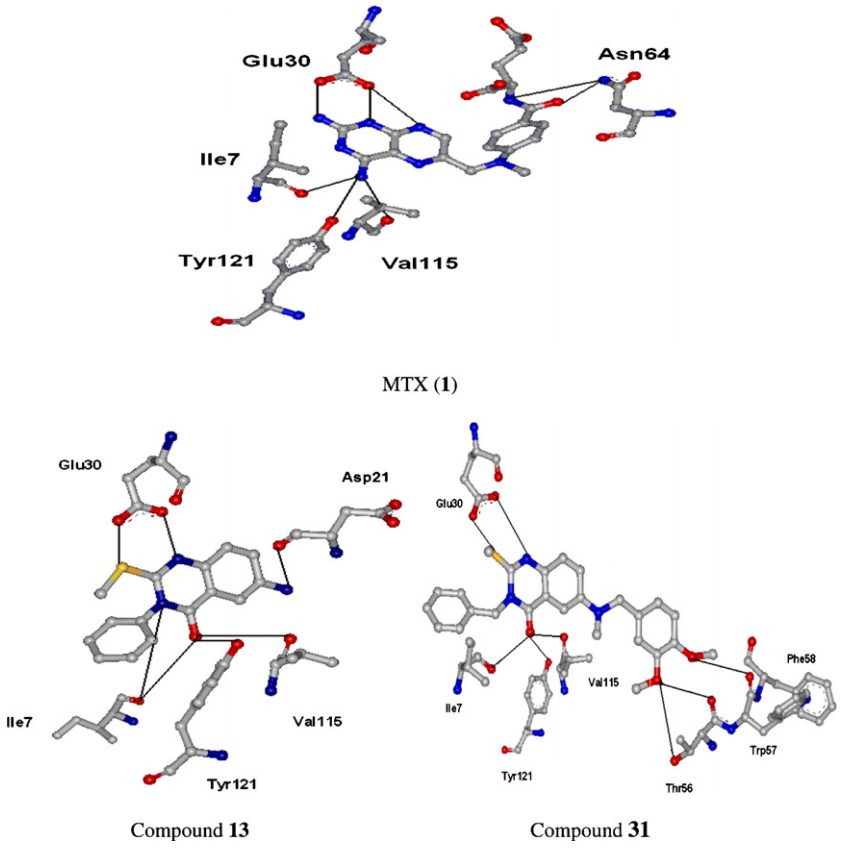

Figure 4. Binding mode for MTX (**1**), and compounds **13** and **31** docked and minimized in the hDHFR binding pocket, showing residues involved in its recognition. Solid lines indicate the H-bond formation.

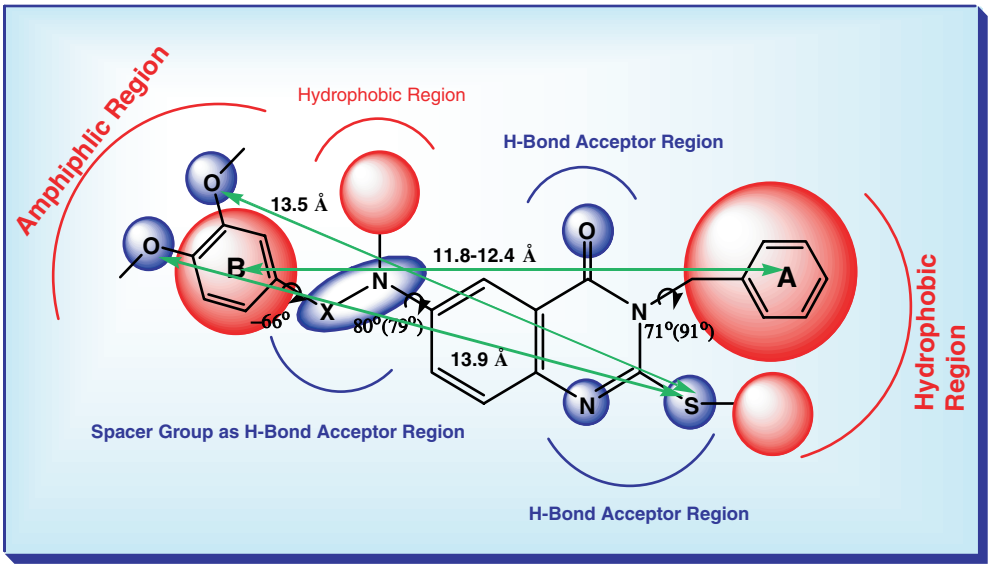

Figure 5. Deduced quinazoline pharmacophore requirement for DHFR binding activity.

formed two H-bonds with Glu30. The 6-amino function of **13** was oriented in the cavity to form H-bond with Asp21, while compound **31** showed three H-bonds with Thr56, Trp57, and Phe58 via the methoxy groups located at positions 3 and 4. Compounds possessing high root mean square deviation (rmsd) values signify a negative correlation with the degree of binding affinity and vice versa. The polar part of the active site appears to be very rigid; the movements of the active site residues upon binding to the tested compounds are limited. This rigidity of the active site is evident from the low rmsd of active site residues in the range of 0.58–1.12.

The structure features essential for the DHFR binding activity of this series (pharmacophore) as determined by the experimental and molecular modeling data are shown in Figure 5. The overall outcome of this molecular docking study revealed that: (i) the quinazoline ring is a satisfactory backbone for inhibitors of mammalian DHFR, establishing contact with the key amino acid residues in the enzyme pocket, (ii) the presence of aryl moiety, ring **A** and ring **B**, at the 3-position and 6-position of quinazoline is necessary for the activity as hydrophobic and amphiphilic regions, respectively, (iii) the two aryl groups at position 3- and 6- should be about 11.8–12.4 Å apart, (iv) The 3-benzyl group favors binding being accommodated within the enzyme binding pocket without steric hindrance as compared to the 3-phenyl substituents, (v) introduction of two atoms spacer group, between quinazoline ring and ring**B**, which contains small hydrophobic alkyl group, enhances the lipophilic interaction with the hydrophobic pocket, such as 6-[*N*-(substituted benzyl)-*N*-methyl-amino]-. Other H-bond acceptor augments the binding interaction within the enzyme pocket, such as 6-[*N*-arylsulfonylamino]-, (vi) the torsional angle between the plane of the quinazoline core and the spacer moiety is 79–80° while in case of MTX (**1**) it is 77°, (vii) the presence of methylthio group located on the 2-position of quinazoline is necessary as H-bond acceptor region to mimic the 2-amino group of **1.** The 2-amino function should be about 13.7 Å apart from the 3,4-dimethoxy groups, which is similar to the non-bonded distance between the 2-amino group of **1** and the carbonyl group of the amide function (Fig. 5), (viii) the 3,4-dimethoxy function improves binding with the active site residues, while the introduction of the third 5-methoxy moiety blunts this interaction, and (ix) the 6-amino group interacts with the surrounding amino acids better than the 7-amino substituents.

3.2. Structure–activity correlation

The obtained DHFR inhibition results revealed that, in the 6-nitro series (**5**–**12**), the 2-SH or 2-SCH_3 moieties do not affect the magnitude of DHFR inhibition as evidenced by the IC_{50} values of the SH containing compounds **5**–**8** and their SCH_3 counterparts **9**–**12**. Reduction of the 6-nitro function into the 6-amino analogs results in variable levels of inhibition. In the 3-phenyl series, reduction of the 6-nitro function decreased the inhibition by 2-fold (**10**, 25.0 μM vs **13**, 50.0 μM); while in the 3-benzyl series, the inhibition increased by 2.5-fold (**11**, 25.0 μM vs **14**, 10.0 μM), in accordance with the molecular modeling predictions. In most cases, moving the 6-nitro group into position-7 did not markedly affect the magnitude of activity. Meanwhile, the translocation of the 6-amino moiety to position-7 reduced the inhibition noticeably (**14**, 10.0 μM vs **15**, 50.0 μM). In the 6-benzylidinamino series (**16**–**21**), the combination of phenyl group at position-3 and 4-methoxy-benzylidinamino at position-6 proved to remarkably enhance the inhibition, as shown in compound **16** (IC_{50} value of 2.0 μM). Replacing the 3-phenyl group of **16** by 3-benzyl moiety decreased the inhibition by 5-fold (**17**, 10.0 μM). The introduction of 3,4-dimethoxy-phenyl replacing the 4-methoxy-phenyl moiety of **16** decreased the inhibition activity by 25-fold (**16**, 2.0 μM vs **18**, 50.0 μM), while the 3,4,5-trimethoxy-phenyl moiety restored some of the DHFR inhibitory potency as shown in compounds **20**

and **21** (IC_{50} 13.0 and 20.0 μM, respectively). Reduction of the 6-benzylidineamino function into the 6-benzylamino analogs (**22**–**27**) showed a slight improvement in DHFR inhibition activity. Upon reductive methylation, using formaldehyde and $NaCNBH_3$ to produce the methotrexate (MTX, **1**) like derivatives (**28**–**33**), the activity increased dramatically producing the most active members in this study (compounds **28**–**32**), which showed IC_{50} values of 1.0, 0.5, 0.4, 0.4, and 1.0 μM, respectively, in accordance with the molecular modeling predictions. In this particular group, the 3-phenyl substitution at the quinazoline nucleus proved to favor the activity, rather than the 3-benzyl, as shown in compound **32** (IC_{50}, 1.0 μM) and the 10-fold decrease in potency in compound **33** (IC_{50}, 10.0 μM). In the 4-substituted benzenesulfonamide series (**34**–**39**), unsubstitution or the presence of 4-bromo moiety favored the activity producing compounds **34** and **36** with IC_{50} value of 2.0 μM for both compounds. The introduction of 4-methyl group to **34** decreased the activity by 5-fold as shown in compound **38** (IC_{50} value of 10.0 μM). In the 6-thioureido series (**40**–**45**), aromatic substitution on the thioureido moiety favored the activity rather than the aliphatic substitution. The *N*-phenyl thioureido substitution proved to be 10-fold more active than the *N*-ethyl analog, as seen in compounds **42** (5.0 μM) and **40** (50.0 μM). In the 6-benzamido series (**46**–**57**), the 3-benzyl substitution as in **49**, **53**, and **55** with IC_{50} values 8.0, 10.0, and 8.0 μM, respectively, favored the activity rather than the 3-phenyl analogs (**48**, **52**, and **54** with IC_{50} values of 50.0, 70.0, and 40.0 μM).

The obtained antitumor testing results revealed that the 7-amino group of **15** (GI_{50}, TGI—34.4, 90.4 μM, respectively) favored the antitumor activity rather than the 6-amino analog **14**. Comparing compound **19** (GI_{50}, TGI, LC_{50}—20.0, 68.0, and 97.8 μM, respectively) with 3,4-dimethoxyphenyl substitution to the inactive 4-methoxy (**17**) and 3,4,5-trimethoxy (**21**) compounds showed that the number and setting of the methoxy groups proved crucial for antitumor activity. For DHFR inhibition, aromatic substitution rather than aliphatic substitution on the thioureido function was favored but the opposite was true for anticancer activity: compound **41** (GI_{50}, TGI, and LC_{50}—26.7 74.7, 97.8 μM, respectively) with its 6-ethylthioureido function was active but compounds **43** and **45**, with aromatic substitution were inactive. The 6-benzamido analog **47** (GI_{50}, TGI, LC_{50}—9.1, 39.5, and 78.1 μM, respectively) represents another example of the effect of substituent on activity in this study. Introduction of the electron-withdrawing bromine atom to **47** or electron-donating methyl function produced compounds **49** and **51**, respectively, with total loss of activity.

4. Conclusion

Compounds **29**, **30**, and **31** are the most active members of this study as DHFR inhibitors with IC_{50} values of 0.5, 0.4, and 0.4 μM, respectively. Compounds **19** (GI_{50}, TGI, and LC_{50} values of 20.1, 68.0, 97.8 μM, respectively): **31** (GI_{50}, TGI, and LC_{50} values of 23.5, 83.1, <100.0 μM, respectively), **41** (GI_{50}, TGI, and LC_{50} values of 26.7, 74.7, and 97.8 μM, respectively); and **47** (GI_{50}, TGI, and LC_{50} values of 9.1, 39.5, and 78.1 μM, respectively) are the most active antitumor agents in this study, as compared with the known antitumor drug 'Melphalan' (GI_{50}, TGI, and LC_{50} values of 27.1, 35.3, and 65.5 μM, respectively). It seemed that compound **31** exerts its antitumor potency through DHFR inhibition mode of action, while the other active compounds, namely **19**, **41**, and **47**, might exert their antitumor potency through DHFR inhibition and/or some other mechanism of action. Some of the differences between DHFR inhibitory activity and whole cell antitumor assays can be related to the ability of the compounds to be taken up by cells or concentrated therein. The comparison of the molecular parameters of compound **31** and MTX (**1**) has led to a great deal of model similarity for this new class of DHFRI. This model suggests that key elements are in common between **1** and the new quinazoline analogs which are stabilized within the active site of the enzyme through hydrophobic and H-bond interaction. Finally, EPS (electrostatic potential isosurface) maps of both compounds **1** and **31** were obtained. The two molecules showed matching regions of high and low electrostatic potential due to their structural resemblance. The results of the computer modeling experiments indicate striking similarities in the mode and strength of binding of the two compounds due to their similar steric, volume, and EPS maps. These studied quinazoline analogs could be considered as useful templates for future development and further derivatization or modification to obtain more potent DHFR inhibitors.

5. Experimental

Melting points (°C) were determined on Mettler FP80 melting point elemental analyzer at the Central Research Laboratory, College of Pharmacy, King Saud University. All of the new compounds were analyzed for C, H, and N, and agreed with the proposed structures within ±0.4% of the theoretical values. ^{1}H and ^{13}C-NMR spectra were recorded on a Varian XL 500 MHz FT spectrometer, chemical shifts are expressed in δ parts per million with reference to TMS. Mass spectral (MS) data were obtained on a Shimadzu GC/MS QP 5000 apparatus. Thin-layer chromatography was formed on precoated (0.25 mm) silica gel GF_{254} plates (E. Merck, Germany), compounds were detected with 254 nm UV lamp. Silica gel (60–230 mesh) was employed for routine column chromatography separations. DHFR inhibition activity experiments were formed at Pharmacology Department, College of Pharmacy, King Saud University. Bovine liver DHFR enzyme and methotrexate (MIX, **3**) were used in the assay (Sigma Chemical Co., USA). Antitumor activity was formed at the National Cancer Institute (NCI), Bethesda, Maryland, USA. Compounds **7** and **11** were previously reported.[33]

All modeling studies were conducted with Hyperchem 6.03 package from Hypercube.[39] Molecular dynamics studies were formed using Amber force field[40,41] within Hyperchem 6.03. The docking of the candidates into

hDHFR pocket was formed with docking protocol in Hyperchem 6.03. Starting coordinate of hDHFR enzyme in tertiary complex with reduced-nicotinamide adenine dinucleotide phosphate (NADPH) and MTX (**3**), code ID 1DLS, was obtained from the Protein Data Bank of Brookhaven National Laboratory.[28]

5.1. 2-Thioxo-3-substituted-6 or 7-nitro-3*H*-quinazolin-4-ones (5, 6, and 8)

A mixture of 4- or 5-nitroanthranilic acid (**4a**,**b**, 1.82 g, 0.01 mol), the appropriate isothiocyanate derivative (0.012 mol), and TEA (2 mL) in ethanol (50 mL) was heated under reflux for 4 h. The reaction mixture was then cooled and the solvent was evaporated under vacuum. The obtained residue was washed with petroleum ether 40:60, filtered, dried and recrystallized to give **5**, **6** and **8** (Table 1). ^{1}H NMR, **5** ($CDCl_3$): δ 1.24 (t, 3H, J = 7.0 Hz, CH_3CH_2), 3.35 (br s, 1H, SH), 4.41–4.45 (q, 2H, J = 7.0 Hz, CH_3CH_2), 7.49 (d, 1H, J = 9.0 Hz, ArH), 8.50–8.53 (dd, 1H, J = 9.0, 3.0 Hz, ArH), 8.60 (d, 1H, J = 3.0 Hz, ArH). Compound **6** (DMSO-d_6): δ 3.07 (br s, 1H, SH), 6.80 (d, 1H, J = 9.0 Hz, ArH), 7.30–7.58 (m, 5H, ArH), 7.98–7.99 (dd, 1H, J = 9.0, 3.0 Hz, ArH), 8.62 (d, 1H, J = 3.0 Hz, ArH). **8** (DMSO-d_6): δ 3.35 (s, 1H, SH), 5.34 (s, 2H, CH_2Ph), 8.15–8.17 (dd, 1H, J = 9.0, 2.0 Hz, ArH), 8.24 (d, 1H, J = 2.0 Hz, ArH), 8.31 (d, 1H, J = 9.0 Hz, ArH).

5.2. 2-Methylthio-3-substituted-6 or 7-nitro-3*H*-quinazolin-4-ones (9, 10, and 12)

A mixture of the 2-thioxoquinazoline analogs **5**, **6**, or **8** (0.01 mol), methyl iodide (5 mL), and anhydrous potassium carbonate (2 g) in acetone (50 mL) was heated under reflux for 8 h. The separated solid was filtered while hot, washed with acetone, the filtrate was then evaporated, and the obtained residue was dried, and recrystallized to give **9**, **10**, and **12** (Table 1). ^{1}H NMR (DMSO), **9**: δ 1.29 (t, 3H, J = 7.0 Hz, CH_3CH_2), 2.67 (s, 3H, SCH_3), 4.08–4.12 (q, 2H, J = 7.0 Hz, CH_3CH_2), 7.64 (d, 1H, J = 9.0 Hz, ArH), 8.46 (d, 1H, J = 9.0 Hz, ArH), 8.68 (s, 1H, ArH). Compound **10**: δ 2.51 (s, 3H, SCH_3), 7.49–7.60 (m, 5H, ArH), 7.61 (d, 1H, J = 9.0 Hz, ArH), 8.52–8.55 (m, 1H, ArH), 8.71 (s, 1H, ArH). Compound **12**: δ 2.64 (s, 3H, SCH_3), 5.36 (s, 2H, CH_2Ph), 7.29–7.36 (m, 5H, ArH), 8.19 (d, 1H, J = 9.0 Hz, ArH), 8.29 (s, 1H, ArH), 8.33 (d, 1H, J = 9.0 Hz, ArH).

5.3. 2-Methylthio-3-(phenyl or benzyl)-6 or 7-amino-3*H*-quinazolin-4-ones (13–15)

A mixture of the 6 or 7-nitro-quinazoline derivatives **10**, **11** or **12** (0.01 mol), Fe powder prewashed with dilute HCl and water (0.5 g), concentrated HCl (10 mL), in ethanol (50 mL), was heated under reflux for 2 h. Concentrated ammonia solution (5 mL) was added to precipitate Fe salts. The resulting mixture was filtered while hot through Celite. Filtrate was concentrated to give the crude products which were recrystallized to yield compounds **13**–**15** (Table 1). ^{1}H NMR ($CDCl_3$), **13**: δ 2.50 (s, 3H, SCH_3), 5.60 (br s, 2H, NH_2), 7.1–7.17 (m, 2H, ArH), 7.35–7.38 (m, 3H, ArH), 7.39–7.53 (m, 3H, ArH). Compound **14**: δ 2.52 (s, 3H, SCH_3), 5.30 (s, 2H, CH_2Ph), 5.61 (br s, 2H, NH_2), 7.18–7.32 (m, 8H, ArH). Compound **15**: δ 2.52 (s, 3H, SCH_3), 5.12 (s, 2H, CH_2Ph), 6.17 (br s, 2H, NH_2), 6.57 (s 1H, ArH), 6.68 (d, 1H, J = 8.5 Hz, ArH), 7.21–7.34 (m, 5H, ArH), 7.77 (d, 1H, J = 8.5 Hz, ArH).

5.4. 2-Methylthio-3-(phenyl or benzyl)-6-[(substituted)benzylidineamino]-3*H*-quinazolin-4-ones (16–21)

An equimolar amount (0.01 mol) of the 6-aminoquinazoline analogs **13** or **14** and the appropriate methoxybenzaldehyde was dissolved in DMF (30 mL) and heated under reflux for 4 h. Solvent was then removed under reduced pressure. The obtained residue was filtered, washed with water, dried, and recrystallized to afford **16**–**21** (Table 1). ^{1}H NMR (TFA), **16**: δ 2.51 (s, 3H, SCH_3), 3.86 (s, 3H, OCH_3), 7.01 (d, 1H, J = 8.5 Hz, ArH), 7.48–7.59 (m, 5H, ArH), 7.60–7.78 (dd, 4H, J = 8.5, 2.5 Hz, ArH), 7.82 (s, 1H, ArH), 7.94 (d, 1H, J = 8.5 Hz, ArH), 8.69 (s, 1H, CH=N). Compound **17**: δ 2.53 (s, 3H, CH_3), 3.85 (s, 3H, OCH_3), 5.30 (s, 2H, CH_2Ph), 7.09–7.11 (m, 1H, ArH), 7.21–7.35 (m, 6H, ArH), 7.62–7.95 (m, 5H, ArH), 8.71 (s, 1H, CH=N). Compound **18**: δ 2.51 (s, 3H, SCH_3), 3.86 (s, 6H, OCH_3), 7.11 (d, 1H, J = 8.5 Hz, ArH), 7.47–7.78 (m, 10H, ArH), 8.67 (s, 1H, CH=N). Compound **19**: δ 2.52 (s, 3H, SCH_3), 3.87 (s, 6H, OCH_3), 5.32 (s, 2H, CH_2Ph), 7.13 (d, 1H, J = 8.5 Hz, ArH), 7.45–7.81 (m, 9H, ArH), 8.71 (s, 1H, ArH), 8.69 (s, 1H, CH=N). Compound **20**: 2.51 (s, 3H, SCH_3), 3.75 (s, 3H, OCH_3), 3.87 (s, 6H, OCH_3), 7.35 (s, 2H, ArH), 7.43–7.52 (m, 2H, ArH), 7.56–7.62 (m, 3H, ArH), 7.69 (d, 1H, J = 8.5 Hz, ArH), 7.78–7.82 (dd, 1H, J = 8.5, 2.5 Hz, ArH), 7.88 (d, 1H, J = 2.5 Hz, ArH), 8.71 (s, 1H, CH=N). Compound **21**: 2.50 (s, 3H, SCH_3), 3.76 (s, 3H, OCH_3), 3.87 (s, 6H, OCH_3), 5.30 (s, 2H, CH_2Ph), 7.32 (s, 2H, ArH), 7.41–7.53 (m, 2H, ArH), 7.54–7.60 (m, 3H, ArH), 7.65–7.82 (m, 2H, ArH), 7.88 (s, 1H, ArH), 8.70 (s, 1H, CH=N).

5.5. 2-Methylthio-3-(phenyl or benzyl)-6-(substituted benzylamino)-3*H*-quinazolin-4-ones (22–27)

The 2-methylthio-3-(phenyl or benzyl)-6-(substituted benzylidine)amino-3*H*-quinazolin-4-ones (**16**–**21**, 0.01 mol) were dissolved in methanol (50 mL) and stirred. $NaBH_4$ (1.0 g) was added portionwise over a period of 0.5 h and stirred at room temperature for another 2 h. Solvent was removed under reduced pressure. Water (20 mL) was then added, and the undissolved solid was filtered and recrystallized from the appropriate solvent to afford **22**–**27** (Table 1). ^{1}H NMR ($CDCl_3$), **22**: δ 2.42 (s, 3H, SCH_3), 3.72 (s, 3H, OCH_3), 4.27 (d, 2H, J = 5.2 Hz, CH_2Ph), 6.71 (t, 1H, J = 5.2 Hz, NH), 6.89 (d, 1H, J = 8.0, Hz, ArH), 7.03 (s, 2H, ArH), 7.28–7.53 (m, 9H, ArH), **23**: δ 2.50 (s, 3H, SCH_3), 3.72 (s, 3H, OCH_3), 4.26 (d, 2H, J = 5.8 Hz, CH_2Ph), 5.27 (s, 2H, CH_2Ph), 6.88 (t, 1H, J = 5.8 Hz, NH), 6.92 (d, 1H, J = 8.0 Hz, ArH), 7.20 (s, 1H, ArH), 7.28–7.31 (m, 10H, ArH). Compound **24**: δ 2.50 (s, 3H, SCH_3), 3.72 (s, 6H, OCH_3), 4.26 (s, 2H, CH_2Ph), 6.90 (s, 1H,

NH), 6.88 (d, 1H, J = 8.0 Hz, ArH), 7.22–7.35 (m, 10H, ArH). Compound **25**: δ 2.50 (s, 3H, SCH_3), 3.71 (s, 6H, OCH_3), 4.25 (s, 2H, CH_2Ph), 5.28 (m, 3H, CH_2Ph and NH), 6.89–7.38 (m, 11H, ArH). Compound **26**: δ 2.42 (s, 3H, SCH_3), 3.63 (s, 3H, OCH_3), 3.74 (s, 6H, OCH_3), 4.26 (d, 2H, J = 5.5 Hz, CH_2Ph), 6.72–6.75 (m, 3H, NH and ArH), 7.08 (s, 1H, ArH), 7.21–7.23 (m, 1H, ArH), 7.37–7.43 (m, 3H, ArH), 7.52–7.53 (m, 3H, ArH). Compound **27**: 2.41 (s, 3H, SCH_3), 3.62 (s, 3H, OCH_3), 3.75 (s, 6H, OCH_3), 4.27 (d, 2H, J = 5.6 Hz, CH_2Ph), 5.29 (s, 2H, CH_2Ph), 6.71–6.76 (m, 3H, NH and ArH), 7.08–7.23 (m, 2H, ArH), 7.38–7.54 (m, 6H, ArH).

5.6. 2-Methylthio-3-(phenyl or benzyl)-6-[N-(substituted benzyl)-*N*-methylamino]-3*H*-quinazolin-4-ones (28–33)

To a solution of 2-methylthio-3-(phenyl or benzyl)-6-(substituted benzylamino)-3*H*-quinazoline-4-ones (**22**–**27**, 0.05 mol) in 50 mL of acetonitrile, formaldehyde (4 g, 0.11 mol) was added with constant stirring. To this suspension, $NaCNBH_3$ (5 g, 0.08 mol) was added, and the pH of the mixture was adjusted to 2–3 using concentrated HCl. Five minutes later a bright yellow precipitate was obtained. The acetonitrile was evaporated under reduced pressure and the obtained residue was suspended in 10 mL of water and neutralized using NH_4OH to afford **28**–**33** which were filtered, dried, and recrystallized (Table 1). ^{1}H NMR (DMSO-d_6), **28**: δ 2.43 (s, 3H, SCH_3), 3.09 (s, 3H, NCH_3), 3.72 (s, 3H, OCH_3), 4.61 (s, 2H, CH_2Ph), 6.88 (d, 2H, J = 8.5 Hz, ArH), 7.13–7.17 (m, 3H, ArH), 7.34–7.38 (m, 3H, ArH), 7.48–7.54 (m, 4H, ArH). Compound **29**: δ 2.40 (s, 3H, SCH_3), 2.98 (s, 3H, NCH_3), 3.71 (s, 3H, OCH_3), 4.51 (s, 2H, CH_2Ph), 5.08 (s, 2H, CH_2Ph), 6.87 (d, 2H, J = 8.5 Hz, ArH), 7.07–7.13 (m, 4H, ArH), 7.22–7.32 (m, 6H, ArH). Compound **30**: δ 2.43 (s, 3H, SCH_3), 3.11 (s, 3H, NCH_3), 3.71 (s, 6H, OCH_3), 4.60 (s, 2H, CH_2Ph), 6.68 (d, 1H, J = 8.0 Hz, ArH), 6.85–6.88 (m, 2H, ArH), 7.16 (d, 1H, J = 3.0 Hz, ArH), 7.36–7.40 (m, 3H, ArH), 7.48–7.56 (m, 4H, ArH). Compound **31**: 2.55 (s, 3H, SCH_3), 3.11 (s, 3H, NCH_3), 3.71 (s, 6H, OCH_3), 4.62 (s, 2H, CH_2Ph), 5.33 (s, 2H, CH_2Ph), 6.71 (s, 1H, ArH), 6.89–6.91 (m, 2H, ArH), 7.19 (s, 1H, ArH), 7.41–7.45 (m, 3H, ArH), 7.51–7.57 (m, 4H, ArH). Compound **32**: δ 2.43 (s, 3H, SCH_3), 3.13 (s, 3H, NCH_3), 3.62 (s, 3H, OCH_3), 3.70 (s, 6H, OCH_3), 4.60 (s, 2H, CH_2Ph), 6.52 (s, 2H, ArH), 7.18 (d, 1H, J = 2.5 Hz, ArH), 7.37–7.40 (s, 3H, ArH), 7.50–7.55 (s, 4H, ArH). Compound **33**: δ 2.56 (s, 3H, SCH_3), 3.13 (s, 3H, NCH_3), 3.63 (s, 3H, OCH_3), 3.70 (s, 6H, OCH_3), 4.60 (s, 2H, CH_2Ph), 5.31 (s, 2H, CH_2Ph), 6.54 (s, 2H, ArH), 7.22–7.46 (m, 8H, ArH).

5.7. 2-Methylthio-3-(phenyl or benzyl)-6-[(substituted phenyl)sulfonyl]amino-3*H*-quinazolin-4-ones (34–39)

A solution of the 6-aminoquinazoline analog **13** or **14** (0.002 mol) and the appropriate phenylsulfonyl chloride derivative (0.003 mol) in pyridine (10 mL) was heated under reflux for 1 h. Solvent was evaporated under reduced pressure and the remaining residue was then triturated with water and filtered. The obtained solid was dried, and recrystallized to give **34**–**39** (Table 2). ^{1}H NMR (DMSO-d_6), **34**: δ 2.43 (s, 3H, SCH_3), 7.28–7.98 (m, 13H, ArH), 10.66 (s, 1H, NH). **35**: δ 2.54 (s, 3H, SCH_3), 5.32 (s, 2H, CH_2Ph), 7.19–7.98 (m, 13H, ArH), 10.69 (br s, 1H, NH). Compound **36**: δ 2.43 (s, 3H, SCH_3), 7.29–7.80 (m, 12H, ArH), 10.72 (br s, 1H, NH). Compound **37**: δ 2.54 (s, 3H, SCH_3), 5.31 (s, 2H, CH_2Ph), 7.19–7.79 (m, 13H, ArH and NH). Compound **38**: δ 2.33 (s, 3H, CH_3Ar), 2.44 (s, 3H, SCH_3), 7.28–7.86 (m, 12H, ArH), 10.54 (br s, 1H, NH). Compound **39**: δ 2.32 (s, 3H, CH_3Ar), 2.54 (s, 3H, SCH_3), 5.28 (s, 2H, CH_2Ph), 5.61 (br s, 1H, NH), 7.07–7.78 (m, 12H, ArH).

5.8. N-Substituted-*N*′-[2-methylthio-3-(phenyl or benzyl)-4-oxo-3*H*-quinazolin-6-yl]-thioureas (40–45)

A solution of the 6-aminoquinazoline derivative **13** or **14** (0.002 mol), and the appropriate isothiocyanate (0.0022 mol) in ethanol (10 mL) was heated under reflux for 6 h. The separated solid was filtered, dried and recrystallized to yield **40**–**45** (Table 2). ^{1}H NMR (DMSO-d_6), **40**: δ 1.15 (t, 3H, CH_2CH_3), 2.43 (s, 3H, SCH_3), 3.45–3.51 (m, 2H, CH_2CH_3), 4.34 (br s, 1H, NH), 5.58 (br s, 1H, NH), 7.18–8.17 (m, 8H, ArH). Compound **41**: δ 1.19 (t, 3H, CH_2CH_3), 2.43 (s, 3H, SCH_3), 3.46–3.49 (m, 2H, CH_2CH_3), 5.37 (s, 2H, CH_2Ph), 6.31 (br s, 1H, NH), 7.28–8.03 (m, 8H, ArH), 8.18 (br s, 1H, NH). Compound **42**: δ 2.49 (s, 3H, SCH_3), 7.27–7.60 (m, 11H, ArH), 7.94 (s, 1H, ArH), 8.22 (s, 1H, ArH), 8.35 (br s, 1H, NH), 9.89 (br s, 1H, NH). Compound **43**: δ 2.59 (s, 3H, SCH_3), 5.34 (s, 2H, CH_2Ph), 7.15 (t, 1H, ArH), 7.24–7.28 (m, 3H, ArH), 7.33–7.37 (m, 4H, ArH), 7.49 (d, 2H, J = 7.5 Hz, ArH), 7.57 (d, 1H, J = 9.0 Hz, ArH), 7.94–7.96 (dd, 1H, J = 9.0, 2.5 Hz, ArH), 8.26 (d, 1H, J = 2.5 Hz, ArH), 10.00 (br s, 1H, NH), 10.08 (br s, 1H, NH). Compound **44**: δ 2.49 (s, 3H, SCH_3), 4.78 (s, 2H, CH_2Ph), 7.27–7.60 (m, 11H, ArH), 7.94 (d, 1H, J = 9.0 Hz, ArH), 8.22 (s, 1H, ArH), 8.35 (br s, 1H, NH), 8.89 (br s, 1H, NH). Compound **45**: δ 2.53 (s, 3H, SCH_3), 5.30 (s, 2H, CH_2Ph), 5.61 (s, 2H, CH_2Ph), 7.06–7.11 (dd, 2H, J = 9.0, 2.5 Hz, ArH), 7.19–7.37 (m, 13H, ArH and NH).

5.9. 2-Methylthio-3-(phenyl or benzyl)-6-[(substituted phenyl)carbonylamino]-3*H*-quinazolin-4-ones (46–57)

A solution of the 6-aminoquinazoline derivative **13** or **14** (0.022 mol) and the appropriate benzoyl chloride analog (0.003 mol) in pyridine (10 mL) was heated under reflux for 1 h and continued as mentioned under **34**–**39** to produce the N-acylated compounds **46**–**57** (Table 2). ^{1}H NMR (DMSO-d_6), **46**: δ 2.50 (s, 3H, SCH_3), 7.31–7.72 (m, 10H, ArH), 8.01 (d, 1H, J = 7.0 Hz, ArH), 8.28 (d, 1H, J = 7.5 Hz, ArH), 8.58 (s, 1H, ArH), 10.59 (br s, 1H, NH). Compound **47**: δ 2.50 (s, 3H, SCH_3), 5.36 (s, 2H, CH_2Ph), 7.22–7.36 (m, 5H, ArH), 7.51–7.65 (m, 5H, ArH), 7.98–8.01 (m, 1H, ArH), 8.20 (dd, 1H, J = 9.0, 2.5 Hz, ArH), 8.64 (d, 1H, J = 2.5 Hz, ArH), 10.59 (s, 1H, NH). Compound **48**: δ 2.52 (s, 3H, SCH_3), 5.31 (br s, 1H, NH), 7.05–7.36 (m, 12H, ArH).

Compound **49**: δ 2.51 (s, 3H, SCH_3), 5.54 (s, 2H, CH_2Ph), 7.00–7.51 (m, 12H, ArH), 12.82 (br s, 1H, NH). Compound **50**: δ 2.40 (s, 3H, CH_3Ph), 2.51 (s, 3H, SCH_3), 7.32–7.69 (m, 9H, ArH), 7.88–7.97 (m, 1H, ArH), 8.23–8.32 (m, 1H, ArH), 8.56 (s, 1H, ArH), 10.46 (s, 1H, NH). Compound **51**: δ 2.40 (s, 3H, CH_3Ph), 2.51 (s, 3H, SCH_3), 5.36 (s, 2H, CH_2Ph), 7.22–7.31 (m, 3H, ArH), 7.33–7.39 (m, 4H, ArH), 7.62 (d, 1H, J = 8.5 Hz, ArH), 7.92 (d, 2H, J = 8.5 Hz, ArH), 8.19–8.25 (dd, 1H, J = 8.5, 2.5 Hz, ArH), 8.65 (d, 1H, J = 2.5 Hz, ArH), 10.50 (br s, 1H, NH). Compound **52**: δ 2.49 (s, 3H, SCH_3), 3.89 (s, 3H, OCH_3), 6.82–7.18 (m, 2H, ArH), 7.40–7.68 (m, 6H, ArH), 7.86–8.12 (m, 3H, ArH), 8.27 (d, 1H, J = 8.5 Hz, ArH), 8.56 (s, 1H, ArH), 10.40 (br s, 1H, ArH). Compound **53**: δ 2.50 (s, 3H, SCH_3), 3.86 (s, 3H, OCH_3), 5.36 (s, 2H, CH_2Ph), 7.09 (d, 2H, J = 9.0 Hz, ArH), 7.24–7.37 (m, 5H, ArH), 7.61 (d, 1H, J = 9.0 Hz, ArH), 8.01 (d, 2H, J = 8.5 Hz, ArH), 8.21–8.23 (dd, 1H, J = 8.5, 2.5 Hz, ArH), 8.62 (d, 1H, J = 2.5 Hz, ArH), 10.43 (s, 1H, NH). Compound **54**: δ 2.49 (s, 3H, SCH_3), 3.86 (s, 6H, OCH_3), 7.10–7.12 (m, 2H, ArH), 7.45–7.69 (m, 7H, ArH), 8.27–8.29 (m, 1H, ArH), 8.53–8.54 (m, 1H, ArH), 10.37 (br s, 1H, NH). Compound **55**: δ 2.50 (s, 3H, SCH_3), 3.86 (s, 6H, OCH_3), 5.36 (s, 2H, CH_2Ph), 7.11 (d, 1H, J = 8.5 Hz, ArH), 7.25–7.34 (m, 3H, ArH), 7.58–7.68 (m, 5H, ArH), 8.23 (d, 1H, J = 8.5 Hz, ArH), 8.60 (s, 1H, ArH), 10.40 (s, 1H, NH). Compound **56**: δ 2.49 (s, 3H, SCH_3), 3.75 (s, 3H, OCH_3), 3.89 (s, 6H, OCH_3), 7.35 (s, 2H, ArH), 7.46–7.49 (m, 2H, ArH), 7.56–7.59 (m, 3H, ArH),7.67 (d, 1H, J = 9.0 Hz, ArH), 8.23–8.31 (m, 1H, ArH), 8.52 (d, 1H, J = 2.5 Hz, ArH), 10.42 (s, 1H, NH). Compound **57**: δ 2.50 (s, 3H, SCH_3), 3.75 (s, 3H, OCH_3), 3.89 (s, 6H, OCH_3), 5.35 (s, 2H, CH_2Ph), 7.22–7.31 (m, 2H, ArH), 7.33–7.41 (m, 5H, ArH), 7.51 (d, 1H, J = 9.0 Hz, ArH), 8.17–8.25 (dd, 1H, J = 9.0, 2.5 Hz, ArH), 8.53 (d, 1H, J = 2.5 Hz, ArH), 10.45 (s, 1H, NH).

5.10. Dihydrofolate reductase (DHFR) inhibition assay

The assay mixture contained 50 mM Tris–HCl buffer (pH 7.4), 50 μM NADPH, 20 μL DMSO or the same volume of DMSO solution containing the test compounds to a final concentration of 10^{-11}–10^{-5} M, and 0.02 U of bovine liver DHFR, in a final volume of 2.0 mL. After addition of the enzyme, the mixture was incubated at room temperature for 2.0 min, and the reaction was initiated by adding 25 μM dihydrofolic acid, the change in absorbance (ΔA/min) was measured at 340 nm. The activity under these conditions was linear for 10 min.[16] Results are reported as % inhibition of enzymatic activity calculated using the following formula:

$$\%\ \text{inhibition} = \left(1 - \frac{\Delta A/\text{min}_{\text{test}}}{\Delta A/\text{min}_{\text{DMSO}}}\right) \times 100$$

The % inhibition values were plotted versus drug concentration (log scale). The 50% inhibitory concentration (IC_{50}) of each compound was obtained. Inhibition plot of MTX (**1**) was also formed showing IC_{50} value of 0.006 μM.

5.11. Molecular dynamics calculations

5.11.1. Enzyme structure. Starting coordinate of hDHFR enzyme in tertiary complex with reduced-nicotinamide adenine dinucleotide phosphate (NADPH) and MTX (**1**), code ID 1DLS, was obtained from the Protein Data Bank of Brookhaven National Laboratory. The structure of human DHFR was the L22Y mutant enzyme in complex with NADPH and methotrexate (PDB entry 1DLS) from which the wild type enzyme was modeled prior to simulation.[28] All the hydrogens were added and enzyme structure was subjected to a refinement protocol in which the constraints on the enzyme were gradually removed and minimized until the rms gradient was 0.01 kcal/mol Å. The energy minimization was carried out using the molecular mechanics force field 'AMBER.' The energy-minimized structure was used for molecular dynamics studies.

5.11.2. Molecular structure of the synthesized quinazolines. The quinazoline analogs **5**–**57** were constructed from fragment libraries in the Hyperchem program.[39] The partial atomic charges for each analog were assigned with the semiempirical mechanical calculation method 'AM1'[40,41] implemented in Hyperchem 6.03. Conformational search was formed around all the rotatable bonds with an increment of 10° using conformational search module as implemented in HyperChem 6.03. All the conformers were minimized until the rms deviation was 0.01 kcal/mol Å.

5.11.3. Docking and molecular dynamics simulations. The docking and MD simulations were carried out on the hDHFR enzyme for each compound. The active site of the enzyme was defined using a radius of 12.0 Å around MTX (**1**).MD simulations were carried out for each ligand, with the rest of the enzyme kept fixed. Non-standard charges of NADPH as a part of the enzyme structure were not fixed during the simulations. The lowest energy conformer 'global-minima' was prepositioned using the crystal structure ligand 'MTX' as a template for the initial placement at the enzyme-binding domain using a flexible fitting of the selected atoms within the MTX ligand. Distance between the hydrogen bond donor and acceptor atoms within the pocket surrounding the ligand and the ligand itself was defined and restrained. Once prepositioned, MTX was deleted and each inhibitor was optimally docked in the enzyme-binding pocket. For each of the quinazoline analogs, energy minimizations (EM) were formed using 1000 steps of steepest descent, followed by conjugate gradient minimization to a RMS energy gradient of 0.01 kcal/mol Å. MD simulation was formed using time steps of 0.001 pico-second (ps), a distance dependent dielectric of 4.00, and a non-bonded cut-off distance of 8.0 Å at 300 K. Complexes were first equilibrated for 10 ps and then simulated for 90 ps. Trajectory frames were collected every 200 steps for detailed analysis on the basis of potential energy, hydrogen bond interactions, and rms deviation of the active site residues were

determined. Energy of binding was calculated as the difference between the energy of the complex and individual energies of the enzyme and ligand:

$$E_{\text{binding}} = E_{\text{Complex}} - (E_{\text{Ligand}} + E_{\text{enzyme}}).$$

where E_{Complex} is the energy of the ligand-enzyme complex, E_{Ligand} is the energy of the ligand corresponding to the binding conformation, and E_{enzyme} is the energy of the enzyme.[40] The conformational energy difference ($<E$) was calculated as the difference between the energy of the conformation within the active site and the energy of the global minimum conformation for each compound. Root-mean-square deviation (rmsd) values of active-site residues were determined as a validation for the nature and flexibility of the active site.

Acknowledgments

The financial support of King Abdulaziz City for Science and Technology, Grant AT-12-18, is acknowledged. Thanks are due to the NCI, Bethesda, MD, for performing the antitumor testing of the synthesized compounds. The technical assistance of Mr. Tanvir A. Butt is greatly appreciated.

References and notes

1. Masur, H. *J. Infect. Dis.* **1990**, *161*, 858–864.
2. Berman, E. M.; Werbel, L. M. *J. Med. Chem.* **1991**, *34*, 479–485.
3. Roth, B. *Fed. Proc.* **1986**, *45*, 2665–2772.
4. Jolivet, J.; Cowan, K. H.; Curt, G. A.; Clendninn, N. J.; Chabner, B. A. *N. Eng. J. Med.* **1983**, *309*, 1094–1104.
5. Borst, P.; Quellette, M. *Annu. Rev. Microbiol.* **1995**, *49*, 427–460.
6. Kozarek, R. A.; Patterson, D. J.; Gelfand, M. D.; Botoman, V. A.; Ball, T. J.; Wilske, K. R. *Ann. Intern. Med.* **1989**, *110*, 353–356.
7. Weinblatt, M. E.; Coblyn, J. S.; Fox, D. A.; Fraser, P. A.; Holdsworth, D. E.; Glass, D. N.; Trentham, D. E. *N. Eng. J. Med.* **1985**, *312*, 818–822.
8. Weinstein, G. D.; Frost, P. *Arch. Dermatol.* **1971**, *103*, 33–38.
9. Abu-Shakra, M.; Gladman, D. D.; Thorne, J. C.; Long, J.; Gough, J.; Faresell, V. T. *J. Rheumatol.* **1995**, *22*, 241–245.
10. Mullarkey, M. F.; Blumenstein, B. A.; Andrade, W. P.; Bailey, G. A.; Olason, I.; Wetzel, C. E. *N. Eng. J. Med.* **1988**, *318*, 603–607.
11. Maroun, J. *Semin. Oncol.* **1988**, *15*, 17–21.
12. Lin, J. T.; Cashmore, A. R.; Baker, M.; Dreyer, R. N.; Ernstoff, M.; Marsh, J. C.; Bertino, J. R.; Whitfield, L. R.; Delap, R.; Griloo-Lopez, A. *Cancer Res.* **1987**, *47*, 609–616.
13. Kovacs, J. A.; Allegra, C. A.; Swan, J. C.; Drake, J. C.; Parillo, J. E.; Chabner, B. A.; Masur, H. *Antimicrob. Agents Chemother.* **1988**, *43*, 430–433.
14. Allegra, C. J.; Chanber, B. A.; Tuazon, C. U.; Ogata Arakaki, D.; Baird, B.; Darke, J. C.; Simmons, J. T.; Lack, E. E.; Shelhamer, J. H.; Balis, F.; Walker, R.; Kovacs, J. A.; Cliffordlane, H.; Masur, H. *N. Eng. J. Med.* **1987**, *317*, 978–985.
15. El-Subbagh, H. I.; El-Sherbeny, M. A.; Nasr, M. N.; Goda, F. E.; Badria, F. A. *Boll. Chim. Farm.* **1995**, *134*, 80–84.
16. Pignatello, R.; Spampinato, G.; Sorrenti, V.; Vicari, L.; Giacomo, C. Di.; Vanella, A.; Puglisi, G. *Pharm. Pharmacol. Commun.* **1999**, *5*, 299–304.
17. Wyss, P. C.; Gerber, P.; Hartman, P. G.; Hubschwerlen, C.; Locher, H.; Marty, H.; Stahl, M. *J. Med. Chem.* **2003**, *46*, 2304–2312.
18. Rastelli, G.; Pacchioni, S.; Sirawaraporn, W.; Sirawaraporn, R.; Parenti, M. D.; Ferrari, A. M. *J. Med. Chem.* **2003**, *46*, 2834–2845.
19. Gebauer, M. G.; McKinaly, C.; Gready, J. E. *Eur. J. Med. Chem.* **2003**, *38*, 719–728.
20. Donkor, I. O.; Li, H.; Queener, S. F. *Eur. J. Med. Chem.* **2003**, *38*, 605–611.
21. Rosowsky, A.; Chen, H.; Fu, H.; Queener, S. F. *Bioorg. Med. Chem.* **2003**, *11*, 59–67.
22. Zink, M.; Lanig, H.; Troschutz, R. *Eur. J. Med. Chem.* **2004**, *39*, 1079–1088.
23. Pignatello, R.; Guccione, S.; Forte, S.; Giacomo, C.; Sorrenti, V.; Vicari, L.; Barretta, G. U.; Balzano, F.; Puglisi, G. *Bioorg. Med. Chem.* **2004**, *12*, 2951–2964.
24. Raffa, D.; Edler, M. C.; Daidone, G.; Maggio, B.; Merickech, M.; Plescia, S.; Schillaci, D.; Bai, R.; Hamel, E. *Eur. J. Med. Chem.* **2004**, *39*, 299–304.
25. Foye, W. O.; Lemke, T. L.; Williams, D. A. *Principles of Medicinal Chemistry*, 2nd ed.; Williams and Wilkins: Media, PA, 2002.
26. Masur, H.; Polis, M. A.; Tuazon, C. V.; Ogota, A. D.; Kovacs, J.; Katz, D.; Hilt, D.; Simmons, T.; Feuerstein, I.; Lundgren, B.; Lane, H. C.; Chabner, B. A.; Allegra, J. C. *J. Infect. Dis.* **1993**, *167*, 1422–1426.
27. Nordberg, M. G.; Kolmodin, K.; Aqvist, J.; Queener, S. F.; Hallberg, A. *J. Med. Chem.* **2001**, *44*, 2391–2402.
28. Nordberg, M. G.; Kolmodin, K.; Aqvist, J.; Queener, S. F.; Hallberg, P. *Eur. J. Pharm. Sci.* **2004**, *22*, 43–53.
29. Abdel Hamid, S. G.; El-Obaid, H. A.; Al-Majed, A. A.; El-Kashef, H. A.; El-Subbagh, H. I. *Med. Chem. Res.* **2001**, *10*, 378–389.
30. El-Subbagh, H. I.; Abu-Zaid, S. M.; Mahran, M. A.; Badria, F. A.; Al-Obaid, A. M. *J. Med. Chem.* **2000**, *43*, 2915–2921.
31. Abdel Hamid, S. G.; El-Obaid, H. A.; Al-Rashood, K. A.; Khalil, A. A.; El-Subbagh, H. I. *Sci. Pharm.* **2001**, *69*, 351–366.
32. Khalil, A. A.; Abdel Hamide, S. G.; Al-Obaid, A. M.; El-Subbagh, H. I. *Arch. Pharm. Pharm. Med. Chem.* **2003**, *336*, 95–103.
33. Al-Omar, M. A.; Abdel Hamide, S. G.; Al-Khamees, H. A.; El-Subbagh, H. I. *Saudi Pharm. J.* **2004**, *12*, 63–71.
34. Grever, M. R.; Schepartz, S. A.; Chabner, B. A. *Semin. Oncol.* **1992**, *19*, 622–638.
35. Monks, A.; Scudiero, D.; Skehan, P. *J. Natl. Cancer. Inst.* **1991**, *83*, 757–766.
36. Boyd, M. R.; Paull, K. D. *Drug Rev. Res.* **1995**, *34*, 91–109.
37. Skehan, P.; Storeng, R.; Scudiero, D.; Monks, A.; McMahon, J.; Vistica, D.; Warren, J. R.; Bokesch, H.; Kenney, S.; Boyd, M. R. *J. Natl. Cancer Inst.* **1990**, *82*, 1107–1112.
38. (a) Profeta, S.; Allinger, N. L. *J. Am. Chem. Soc.* **1985**, *107*, 1907–1918; (b) Dosen-Micovic, L.; Jeremic, D.; Allinger, N. L. *J. Am. Chem. Soc.* **1983**, *105*, 1716–1722; (c) Allinger, N. L. *J. Am. Chem. Soc.* **1977**, *99*, 8127–8134.

39. Hyperchem: Molecular Modeling System, Hypercube, Inc., Release 6, Florida, USA, 1999.
40. Cornell, W. D.; Cieplak, P.; Bayly, C. I.; Gould, I. R.; Merz, K. M., Jr.; Ferguson, D. M.; Spellmeyer, D. C.; Fox, T.; Caldwell, J. W.; Kollman, P. A. *J. Am. Chem. Soc.* **1995**, *117*, 5179–5197.
41. Dewar, M. J. S.; Zoebisch, E. G.; Healy, E. F.; Stewart, J. J. P. *J. Am. Chem. Soc.* **1985**, *107*, 3902–3909.
42. Abdel-Aziz, A. A.-M.; El-Subbagh, H. I.; Kunieda, T. *Bioorg. Med. Chem.* **2005**, *13*, 4929–4935, and the references cited therein.
43. Klon, A. E.; Heroux, A.; Ross, L. J.; Pathak, V.; Johnson, C. A.; Piper, J. R.; Borhanti, D. w. *J. Mol. Biol.* **2002**, *320*, 677–682.
44. Gokhale, V. M.; Kulkarni, V. M. *J. Comput. Aided Mol. Des.* **2000**, *14*, 495–506.